Recruitment and Derecruitment during Acute Respiratory Failure

A Clinical Study

STEFANIA CROTTI, DANIELE MASCHERONI, PIETRO CAIRONI, PAOLO PELOSI, GIULIO RONZONI, MICHELE MONDINO, JOHN J. MARINI, and LUCIANO GATTINONI

Istituto di Anestesia e Rianimazione, Università degli Studi di Milano, Ospedale Maggiore Policlinico—IRCCS, Milan, Italy; and Department of Pulmonary and Critical Care Medicine, University of Minnesota, Regions Hospital, St. Paul, Minnesota

In a model of acute lung injury, we showed that positive end-expiratory pressure (PEEP) and tidal volume (V_T) are interactive variables that determine the extent of lung recruitment, that recruitment occurs across the entire range of total lung capacity, and that superimposed pressure is a key determinant of lung collapse. Aiming to verify if the same rules apply in a clinical setting, we randomly ventilated five ALI/ARDS patients with 10, 15, 20, 30, 35, and 45 cm H_2O plateau pressure and 5, 10, 15, and 20 cm H_2O of PEEP. For each PEEP–V_T condition, we obtained computed tomography at end inspiration and end expiration. We found that recruitment occurred along the entire volume–pressure curve, independent of lower and upper inflection points, and that estimated threshold opening pressures were normally distributed (mode = 20 cm H_2O). Recruitment occurred progressively from nondependent to dependent lung regions. Overstretching was not associated with hyperinflation. Derecruitment did not parallel deflation, and estimated threshold closing pressures were normally distributed (mode = 5 cm H_2O). End-inspiratory and end-expiratory collapse were correlated, suggesting a plateau–PEEP interaction. When superimposed gravitational pressure exceeded PEEP, end-expiratory collapse increased. We concluded that the rules governing recruitment and derecruitment equally apply in an oleic acid model and in human ALI/ARDS.

In an experimental model of acute lung injury (oleic acid in dogs), we found that recruitment is a continuous process occurring along the entire inspiratory limb of the volume–pressure (VP) curve of the respiratory system (1). Moreover, we found that the extent of end-expiratory collapse mainly depends on two phenomena: the maximum volume/pressure achieved during the previous inspiration, and the gravitational forces, that is, the superimposed pressure, which compress most dependent lung regions.

Those experimental data were obtained in a model that induces massive pulmonary edema, reversibly collapses 50% of the lung tissue at end expiration, and allows positive pressure to counteract the compressive forces with relative ease.

Acute lung injury (ALI) and the adult respiratory distress syndrome (ARDS) that occur clinically often present a different underlying pathology. We previously found (2) that the pathogenetic pathway producing lung injury (from pulmonary or extrapulmonary cause) may influence the potential for recruitment. Although mixed forms almost certainly exist in practice (3), we hypothesized that the prevalent phenomenon in "primary" ARDS is consolidation—intraalveolar "occupation"—that is relatively insensitive to positive pressure; in ARDS secondary to extrapulmonary causes, the prevalent phenomenon is lung collapse, a condition highly sensitive to positive pressure.

Because the underlying conditions in clinical ALI/ARDS differ so much from the oleic acid model, we wanted to see if in human ALI/ARDS the "rules" for recruitment and derecruitment were similar to those we found in the animal model. We studied five ALI/ARDS patients (one with secondary and four with primary ARDS) and addressed three objectives: (*1*) to document whether recruitment occurs along the entire VP curve, independent of lower and upper inflection points; (*2*) to define the importance of superimposed pressure in the distribution of atelectasis; and (*3*) to describe the possible interactions between end-inspiratory and end-expiratory collapse.

METHODS

The hospital ethical committee granted approval for this study, and informed consent was obtained from the patients' next of kin.

Study Population

We studied five consecutive patients, who had ALI/ARDS according to the criteria suggested by the European American Consensus Conference on ARDS (4). The most relevant demographic and clinical characteristics of the patients are summarized in Table 1. Every patient was intubated and ventilated with a Siemens Servo 900C ventilator in the supine position. Airway pressure was recorded, and arterial and thermodilution catheters were in place, for blood gases, hemodynamic, and physiological measurements.

Experimental Protocol

During the study in a computerized tomography (CT) scan room, the patients were sedated with fentanyl and diazepam, and paralyzed with pancuronium bromide. We employed a Phillips Tomoscan Scanner (Phillips, Eindhoven, The Netherlands), and exposures were taken at 120 kW, 50 mA, and 2 s. After obtaining a frontal tomogram of the chest, the CT scan was positioned at the lung bases in a position such as to avoid the appearance of the diaphragm dome even at the lowest pressures used. The CT scan was limited to one slice to avoid unnecessary X-ray exposure. Before starting the experimental procedure, we constructed a VP curve by supersyringe in each patient.

The experimental procedure is depicted in Figure 1. As shown, the patients were ventilated in pressure control mode at plateau pressures of 30 and 35 cm H_2O (these sequences, indicated as 4 and 5 in Figure 1, were randomized). Each of these plateau pressures was associated with four levels of positive end-expiratory pressure (PEEP): 5, 10, 15, and 20 cm H_2O (the PEEP sequence was also randomized). Each ventilation period with a given plateau—PEEP association lasted approximately 15 min.

At the end of each period, we obtained an inspiratory CT scan at the plateau pressure and an expiratory CT scan at the PEEP (by using the inspiratory and the expiratory hold options of the Siemens 900C, respectively). At the end of each period, we also measured gas exchange (arterial and mixed venous blood), respiratory mechanics, and end-expiratory lung volume (EELV) by the helium dilution technique. Indeed, the available CT scan data were four inspiratory points/patient at 30 cm H_2O and four at 35 cm H_2O. At end expiration

(*Received in original form July 5, 2000 and in revised form January 25, 2001*)

Correspondence and requests for reprints should be addressed to Prof. Luciano Gattinoni, Istituto di Anestesia e Rianimazione, Università degli Studi di Milano, Ospedale Maggiore di Milano—IRCCS, Via Francesco Sforza 35, 20122 Milan, Italy. E-mail: gattinon@polic.cilea.it

Am J Respir Crit Care Med Vol 164. pp 131–140, 2001
Internet address: www.atsjournals.org

TABLE 1. DEMOGRAPHIC AND CLINICAL CHARACTERISTICS

	Patient 1	Patient 2	Patient 3	Patient 4	Patient 5	Mean	SD
Sex, M/F	F	M	M	F	M	3M/2F	
Age, yr	62	19	23	25	29	31.6	17.4
ARDS onset, d	2	1	8	6	6	4.6	3.0
Etiology	Pneumonia	Polytrauma	Hemor. alveol.	Pneumonia	Pneumonia	—	
PEEP, cm H_2O	12	14	11	12	12	12.2	1.1
$F_{I_{O_2}}$, %	80	50	40	50	60	56.0	15.2
$Pa_{O_2}/F_{I_{O_2}}$, mm Hg	122.5	234.0	187.5	202.0	158.3	180.9	42.5
$\dot{V}_E$, L/min	9.0	9.7	8.0	6.2	10.6	8.7	1.7
Pa_{CO_2}, mm Hg	58.9	40.0	52.0	49.0	46.8	49.3	6.9
Cstart, ml/cm H_2O	27.0	35.7	38.5	18.5	14.7	26.9	10.4
Cinf, ml/cm H_2O	48.7	57.1	94.6	41.7	74.0	63.2	21.3
LIP, cm H_2O	9.9	5.7	5.5	11.0	9.6	8.3	2.6
UIP, cm H_2O	25.4	n.d.	n.d.	n.d.	n.d.	—	
Outcome, D/S	D	S	S	S	D	3S/2D	

Definition of abbreviations: ARDS onset = elapsed days from the time at which the ARDS criteria were met and the time of the study; Cinf = compliance of the linear portion of the volume–pressure curve; Cstart = compliance at 100 ml lung inflation; D = died; $F_{I_{O_2}}$ = inspired oxygen fraction; Hemor. alveol. = hemorrhagic alveolitis; LIP = lower inflection point; n.d. = not detected; PEEP = positive end-expiratory pressure; S = survived; UIP = upper inflection point; $\dot{V}_E$ = minute ventilation.

we had one expiratory point/patient at PEEP of 5, 10, 15, and 20 cm H_2O coming from 30 cm H_2O plateau pressure (four points) and one expiratory point/patient at PEEP of 5, 10, 15, and 20 cm H_2O coming from 35 cm H_2O plateau pressure (four points).

The patients were then ventilated (*see* Figure 1, sequence 1, 2, 3, and 6) with 10, 15, 20, and 45 cm H_2O plateau pressure. The plateaus of 10, 15, and 20 were associated with 5 cm H_2O of PEEP. For safety reasons, the CT scans were taken only at plateau pressure and not at end expiration. The plateau pressure of 45 cm H_2O was associated with PEEP of 5, 10, 15, and 20 cm H_2O (randomized sequence). CT scans were taken once at 45 cm H_2O and once at PEEP of 5, 10, 15, and 20 cm H_2O (*see* Figure 1). At the end of the experiment, a CT scan at 0 cm H_2O of PEEP was also taken. Each period of this last part of the study lasted approximately 5 min, to avoid unnecessary hyperventilation or overstretching. For time reasons, in this last part of the study, only CT scan and mechanical measurements were performed. Thus, each patient had the following CT available data: *end inspiration*—four CT scans at plateau pressure of 30 cm H_2O and four at plateau pressure of 35 cm H_2O; one CT scan at plateau pressures of 10, 15, 20, and 45 cm H_2O; *end expiration*—one CT scan at 0 cm H_2O of PEEP, three CT scans at PEEP of 5, 10, 15, and 20 cm H_2O, coming from different plateau pressures (30, 35, and 45 cm H_2O). I/E ratio and respiratory rate were kept constant during the entire study protocol (respectively, 1/2 and 11.6 ± 1.6 breaths/min). No patient showed auto-PEEP during data acquisition.

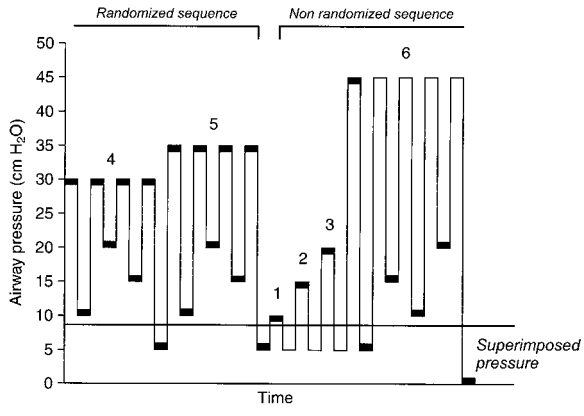

Figure 1. Experimental protocol. Airway pressures at end inspiration (plateau pressure) and at end expiration (positive end-expiratory pressure) as a function of time. The sequences 4 and 5 were randomized and the sequences 1, 2, 3, and 6 were not. The steps in which we performed a computed tomography (CT) scan are marked with a bold line. Solid line at the bottom of the figure represents the mean superimposed pressure computed in these patients at end expiration (8.8 ± 0.7 cm H_2O).

Image Analysis

The procedure for CT scan image analysis has been previously reported (5) and will be summarized here. We analyzed separately the images of the basal CT section of the 10 lungs of the five patients studied. The outline of the basal CT section of each lung was established visually, drawing the outer boundary along the inside of the ribs and the inner boundary along the mediastinal organs. We then arbitrarily divided the total height of the basal CT section into 10 equally spaced levels. Level one refers to the most ventral or nondependent level and level 10 to the most dorsal or dependent level.

The quantitative approach to the CT scan relies on the analysis of the "CT numbers," which substantially define the density (i.e., mass/volume) of each voxel (dimension 0.15 × 0.15 × 0.9 cm) composing the image.

The "CT numbers," expressed in Hounsfield units (HU), range from +1000 HU (bone) to −1000 HU (air), with the water CT number equal to 0 HU. For each CT section and lung level we computed the frequency distribution of the CT numbers, as the frequency of voxels characterized by CT number between −1000 HU and −900 HU; −900 HU and −800 HU; etc. until 0 HU and +100 HU.

Measurements and Definitions

The following variables were measured or computed for each experimental condition:

1. We constructed the static VP curve immediately before the study without previous standardization of lung volume history, using an automatic supersyringe and inflating the lung stepwise (100 ml per step, 2 s intervals), starting from atmospheric pressure up to 1.4 l inflation.
2. We defined total lung capacity of the whole lung (TLC_{WL}) as the end-inspiratory lung volume at a plateau pressure of 45 cm H_2O. TLC_{WL} was computed as the end-expiratory lung volume (EELV) + the tidal volume (V_T) in use, where EELV was measured by a simplified closed-circuit helium method (6).

CT derived variables:

1. We computed the CT gas volume as gas volume = volume × CT/−1000, where the volume is the CT section area (in cm^2) multiplied by the cephalocaudal thickness (0.9 cm), and CT is the mean CT number of the considered area, expressed in HU.
2. We defined total lung capacity of the CT slice (TLC_{CT}) as the gas volume measured in the CT slice at 45 cm H_2O inflation pressure.
3. We defined as "normally aerated" tissue that included voxels between −1000 HU and −500 HU, as "poorly aerated" tissue that included voxels between −500 HU and −100 HU, and as "nonaerated" tissue that included voxels between −100 HU and +100 HU (5). Although the voxels within −100 HU and 0 HU are not strictly gas free (gas tissue ratios between 1/10 and 0), they were included in the nonaerated tissue compartment. In fact, they may represent the small airway collapse in which some gas is left in the pulmonary unit behind the collapsed bronchiolus (7).

4. We estimated "hyperinflation" as the fraction of CT numbers included within −1000 HU and −900 HU, as suggested by Vieira and coworkers (8). This compartment represents gas overfilling (−1000 HU = all gas; −900 HU = gas–tissue ratio of 9/1). Indeed, hyperinflation refers to excessive gas content and not necessarily to overstretching, which relates to the alveolar wall tension. A lung can be overstretched but not overfilled with air (and vice versa).
5. We defined as "superimposed pressure" the gravitational pressure above a given lung level (9), and computed it as the sum of the hydrostatic pressures of the levels above plus the hydrostatic pressure of that level. The hydrostatic pressure of each level was computed as

$$\text{Hydrostatic pressure} = (1 - [\text{CT}/-1000]) \times \text{Ht}$$

where Ht is the height and CT the mean CT number of each level.
6. We defined the transalveolar pressure (10) as the superimposed pressure minus the pressure applied to the airway under static conditions.
7. We defined the "potential for recruitment" as the greatest amount of nonaerated tissue minus the least amount of nonaerated tissue recorded in any given patient. The fractional recruitment for the entire CT slice was expressed as

$$1 - (\text{observed inspiratory nonaerated tissue} - \text{least amount of nonaerated tissue}/\text{potential for recruitment})$$

The fractional recruitment for each level was computed as

$$1 - \text{observed inspiratory nonaerated tissue [level]} - \text{least amount of nonaerated tissue [level]}/\text{potential for recruitment}$$

8. Inflation and recruitment pressure curves were constructed by plotting the inspiratory plateau pressure (x axis) versus the percentage of the TLC_{CT} (inflation pressure curve—y axis) or versus the fractional recruitment (recruitment pressure curve—y axis). As shown in Figure 1, we had available, for each patient, one end-inspiratory CT gas volume or collapse value for the plateau pressures of 10, 15, 20, and 45 cm H_2O, and four end-inspiratory CT gas volume or collapse values for the plateau pressures of 30 and 35 cm H_2O. The four values of end-inspiratory CT gas volume and collapse at 30 and 35 cm H_2O plateau pressures were averaged. Thus, the fraction of TLC_{CT} and recruitment (y axis) refer to one point/patient for the plateau pressures of 10, 15, 20, and 45 cm H_2O, and to the average of four points/patient for the 30 and 35 cm H_2O plateau pressures. Inflation and recruitment pressure curves were fitted with a sigmoid function ($y = a/\{1 + \exp[-(x - x_0)/b]\}$), where a corresponds to the vital capacity, b is a parameter proportional to the pressure range within which most of the volume change takes place, and x_0 is the pressure at the inflection point of the sigmoidal curve (where curvature changes sign), according to Venegas and coworkers (11).
9. We defined estimated "threshold opening pressures" (TOPs) as the pressures at which new increment of recruitment was observed. The data were derived, at 5 cm H_2O pressure intervals, from the fitted recruitment pressure curve obtained in each patient. Thus, data are not strictly experimental but estimate the threshold opening pressures. Frequency distribution of TOPs has been fitted with a gaussian function ($y = a \times \exp\{-0.5\,[(x - x_0)/b]^2\}$).
10. Derecruitment was defined as the amount of poorly and normally aerated tissue that became nonaerated during deflation. The fractional derecruitment for the entire CT slice was expressed as

$$1 - (\text{observed expiratory nonaerated tissue} - \text{least amount of nonaerated tissue/potential for recruitment}).$$

The fractional derecruitment of each level was computed as

$$1 - (\text{observed expiratory nonaerated tissue [level]} - \text{least amount of nonaerated tissue [level]/potential for recruitment}).$$

11. Deflation and derecruitment pressure curves were constructed by plotting the end-expiratory pressures (20, 15, 10, 5, and 0 cm H_2O) versus the corresponding end expiratory CT gas volume—expressed as a fraction of TLC_{CT}—or end-expiratory collapse—expressed as a fraction of potential for recruitment. As shown in the experimental protocol (*see* Figure 1), we had available three end-expiratory CT gas volume and collapse values at 20, 15, 10, and 5 cm H_2O. These values were averaged. At 0 cm H_2O pressure, we had available only one point/patient. Thus, the deflation and derecruitment (y axis) refer to one point/patient at 0 cm H_2O end-expiratory pressure and to an average of three points/patient at pressure of 20, 15, 10, and 5 cm H_2O. Deflation and derecruitment pressure curves were fitted with a sigmoid function ($y = a/\{1 + \exp[-(x - x_0)/b]\}$), where a corresponds to the vital capacity, b is a parameter proportional to the pressure range within which most of the volume change takes place, and x_0 is the pressure at the inflection point of the sigmoidal curve (where curvature changes sign) (11).
12. We defined estimated "threshold closing pressures" (TCPs) as the pressures at which derecruitment was observed. The data were derived at 5 cm H_2O pressure intervals from the fitted derecruitment pressure curve obtained in each patient. Thus, data are not strictly experimental but an estimate of the threshold closing pressures. Frequency distribution of TCPs has been fitted with a gaussian function ($y = a \times \exp\{-0.5\,[(x - x_0)/b]^2\}$).

Statistical Analysis

All data are expressed as mean ± standard error (SEM). Regression analysis was performed with the least-squares method. Values obtained at different levels of PEEP and inspiratory plateau pressure were compared using the two-way analysis of variance (ANOVA) for repeated measures. Individual comparisons were performed using the paired *t* test; Bonferroni's correction was applied for multiple comparisons. Despite the small number of patients, we used a parametric statistic analysis in accordance to the results of Normality and Equal variance test. The data we compared have an approximately gaussian distribution and an equal variance. Significance was accepted as $p < 0.05$.

RESULTS

Potential for Recruitment

As shown in Table 2, the potential for recruitment in this series of patients represented, on average, only 6% of the lung parenchyma.

Inflation and Recruitment

Figure 2 compares the VP curve of the entire lung with the VP curve of the CT slice (VP_{CT}). The VP_{CT}, which covers a pressure range from 0 to 45 cm H_2O, presents a sigmoid shape ($r = 0.99$, $p < 0.0001$) with both lower and upper inflection points. The point by point regression between the volume fractions of the two curves at the same pressure was highly significant ($r = 0.99$, $p < 0.001$, slope = 1.05, y-intercept = 0.0%). Indeed, the similarity of the two curves suggests that the inferences made on the VP_{CT} may be reasonably translated to the entire lung. In Figure 3 (*upper panel*), recruitment is expressed as a function of the inspiratory pressure. Recruitment appears to occur along the entire VP curve, and bears no close correspondence

TABLE 2. POTENTIAL FOR RECRUITMENT

	Potential for Recruitment (*g*)	Total Parenchyma Tissue (*g*)	Potential for Recruitment* (%)
Patient 1	31.7	191.6	17
Patient 2	9.5	209.0	5
Patient 3	5.9	191.8	3
Patient 4	0.8	101.3	1
Patient 5	11.0	174.9	6
Mean	11.8	173.7	6
SD	11.8	42.2	6.2
SEM	5.3	18.9	2.8

* Potential for recruitment, expressed in grams, is normalized for total lung tissue included in the slice, expressed in grams.

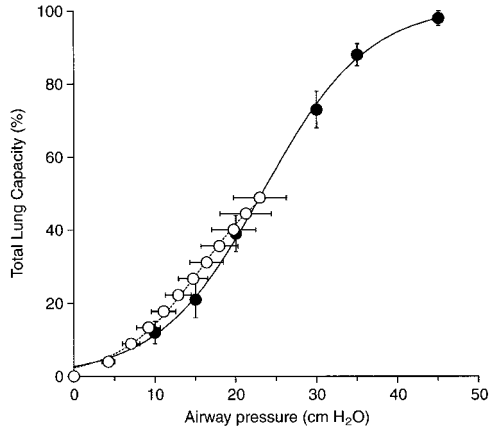

Figure 2. Volume–pressure (VP) curve obtained with the supersyringe technique in the whole lung (*open circles* and *dashed line*) and volume–pressure curve of the lung CT slice (*solid circles* and *solid line*). Volume is expressed as a percentage of total lung capacity. VP whole lung: $r = 0.99$, $p < 0.0001$; VP lung CT slice: $r = 0.99$, $p < 0.0001$.

to either the lower or the upper inflection points. It is also noteworthy that recruitment paralleled inflation; the correlation between percent of inflation and percent of recruitment (not shown) is highly significant and close to identity ($r = 0.99$, $p < 0.001$, slope = 0.91, y-intercept = 0.0%). In the lower panel of Figure 3, the average frequency distribution of the estimated TOPs is reported. This closely fits a gaussian function ($r = 0.90$, $p < 0.01$), and the maximal opening frequency appears around 20 cm H_2O. The estimated TOPs for each patient are reported in Figure 4 (*left side*). As shown, in three patients (patients 1, 3, and 5) the maximal frequency of estimated TOPs was around 20 cm H_2O; in patients 2 and 4 this maximal frequency occurred around 35–40 cm H_2O, explaining the "tail" of the average frequency distribution of estimated TOPs, reported in Figure 3 (*lower panel*).

The regional distribution of recruitment is shown for inspiratory pressures from 0 to 45 cm H_2O in Figure 5. In the first three lung levels (nondependent lung), there is no recruitable tissue; between levels 4 and 7 (middle lung) most recruitment is completed by 30 cm H_2O; between levels 8 and 10 (the most dependent lung regions) recruitment continues up to the highest applied pressure of 45 cm H_2O. Of note, while increasing airway pressure, some regions occasionally show a modest derecruitment, a phenomenon that has previously been observed (7).

Hyperinflation and Overstretching

In Table 3 are reported the CT numbers recorded at inspiratory pressures of 30, 35, and 45 cm H_2O. We did not observe any sign of hyperinflation. In fact, the frequency of voxels with CT numbers between −1000 HU (all gas) and −900 HU (gas tissue ratio of 9/1) was within the range observed in normal subjects (2.1 ± 3%) (12) even at the highest pressure used (45 cm H_2O), a level of pressure at which the VP_{CT} clearly suggests overstretching (*see* Figure 2), that is, increased alveolar wall tension with flattening of the volume–pressure relationship.

Deflation and Derecruitment

Figure 6 shows deflation and derecruitment as functions of expiratory airway pressure. The data points refer to the mean values recorded at a given pressure, during deflation, independent of the previous inspiratory pressure cycling (i.e., we averaged the values obtained at 20, 15, 10, and 5 cm H_2O PEEP,

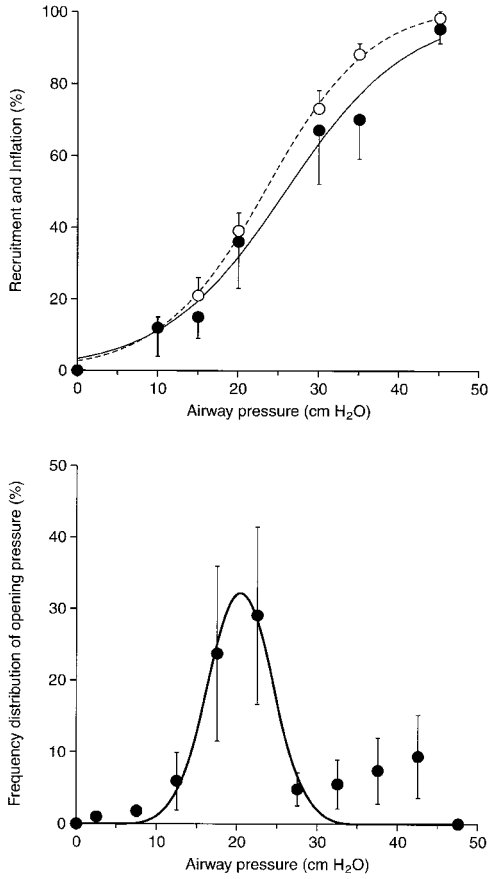

Figure 3. Upper panel: recruitment as a function of airway pressure. *Solid circles* and *solid line* refer to fractional recruitment of the potential for recruitment ($r = 0.99$, $p = 0.0002$); *open circles* and *dashed line* refer to fractional inflation of the lung CT slice ($r = 0.99$, $p < 0.0001$). *Lower panel*: frequency distribution of estimated threshold opening pressures as a function of airway pressure ($r = 0.90$, $p < 0.01$). Each point has been computed at 5 cm H_2O pressure intervals from the fitted recruitment pressure curve obtained in each patient. Thus, these points are not experimental but an estimate of the threshold opening pressures. Data are expressed as mean ± SEM.

regardless of whether they were obtained coming from plateau pressures of 30, 35, or 45 cm H_2O). Both deflation and derecruitment fit a sigmoid function ($r = 0.99$, $p < 0.01$ and $r = 0.98$, $p < 0.01$, respectively). Of note, differently from inspiration, the expiratory lines of deflation and derecruitment are not parallel, suggesting a decrease of gas content without collapse. The frequency distribution of the estimated TCPs is reported in the lower panel of Figure 6, closely fitting a gaussian curve ($r = 0.91$, $p < 0.001$). The maximal frequency of estimated TCPs occurred around 5 cm H_2O; that is, it is shifted to the left, compared to the distribution of the estimated TOPs. This is true for each patient, as shown in Figure 4 (*right side*).

The regional pattern of derecruitment is reported in Figure 7. As shown, the derecruitment is completed down to level 7 at 10 cm H_2O PEEP and, from 10 to 0 cm H_2O PEEP, collapse occurs only in the three most dependent levels (levels 8 to 10). In some regions a paradoxical slight recruitment may be observed when decreasing airway pressure.

End-inspiratory–End-expiratory Pressure Interactions

In Table 4 we report the amount of nonaerated tissue both at end inspiration and at end expiration. As shown, the amount of nonaerated tissue at the end of inspiration tends to de-

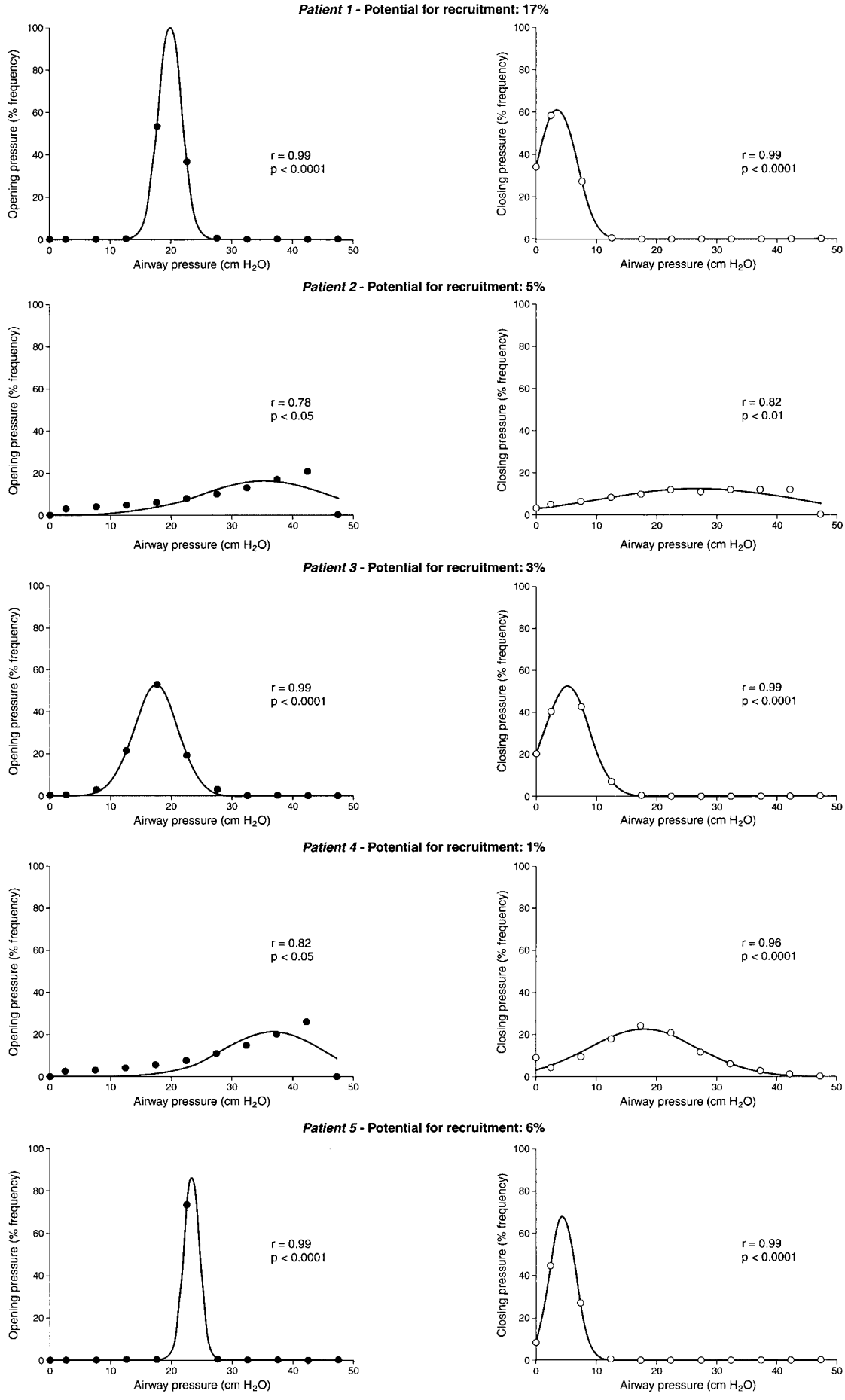

Figure 4. *Left panels*: frequency distribution of estimated threshold opening pressures as a function of airway pressure for each single patient. Each point has been computed at 5 cm H_2O pressure intervals from the fitted recruitment pressure curve obtained in each patient. Thus, these points are not experimental but an estimate of the threshold opening pressures. *Right panels*: frequency distribution of estimated threshold closing pressures as a function of airway pressure for each single patient. Each point has been computed at 5 cm H_2O pressure intervals from the fitted derecruitment pressure curve obtained in each patient.

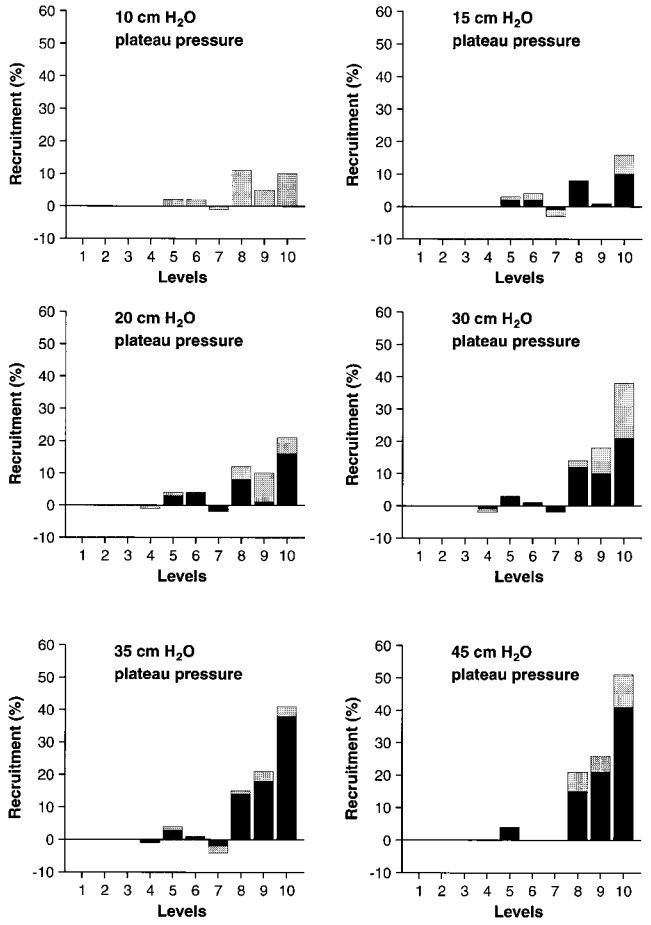

Figure 5. Regional pattern of recruitment. Each graph shows fractional recruitment as a function of lung levels (supine position, level 1 sternal, level 10 vertebral). *Gray bar chart* represents the incremental fractional recruitment at different plateau pressures; *black bar chart* represents the fractional recruitment obtained at the previous plateau pressure. The *black bars* may present a lower value compared with a previous plateau pressure level, meaning a slight regional derecruitment when increasing airway pressure.

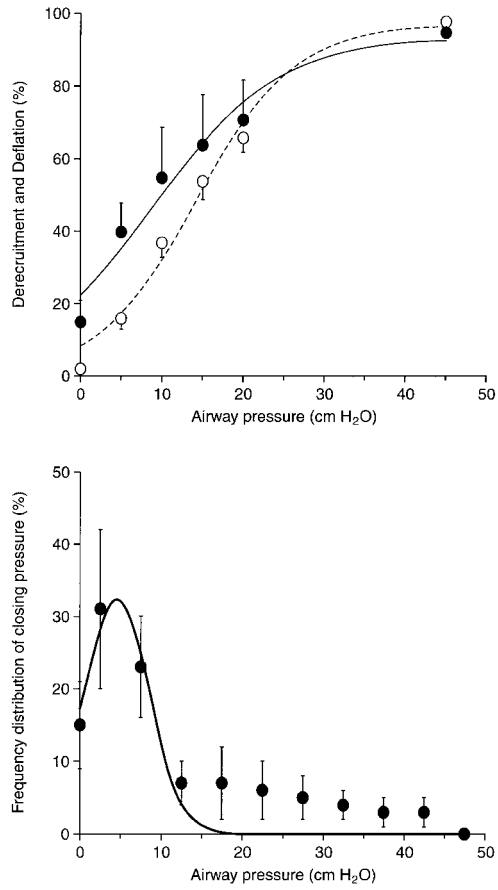

Figure 6. Upper panel: derecruitment as a function of airway pressure. *Solid circles* and *solid line* refer to the fractional derecruitment of the potential for recruitment ($r = 0.98$, $p < 0.01$); *open circles* and *dashed line* refer to the fractional deflation of the lung CT slice ($r = 0.99$, $p < 0.01$). *Lower panel*: frequency distribution of estimated threshold closing pressures as a function of airway pressure ($r = 0.91$, $p < 0.001$). Each point has been computed at 5 cm H_2O pressure intervals from the fitted derecruitment pressure curve obtained in each patient. Thus, these points are not experimental but an estimate of the threshold closing pressures. Data are expressed as mean ± SEM.

crease in the transitions from 30 to 35 to 45 cm H_2O plateau pressure, but the differences did not reach significance. At every PEEP level tested (5, 10, 15, and 20 cm H_2O), the amount of nonaerated tissue at end expiration was significantly less when the expiration followed 45 cm H_2O plateau pressure compared with plateaus of 30 and 35 cm H_2O, as illustrated in Figure 8. The interaction between end inspiration and end expiration is shown in Figure 9, which illustrates that the greater the amount of nonaerated tissue at end inspiration, the greater it is at end expiration ($r = 0.97$, $p < 0.0001$, slope = 1.06, y-intercept = 1.6 g). This dependence suggests that the tissue, which remains open at end expiration, is in part a function of the tissue that has been opened at end inspiration.

TABLE 3. CT NUMBER FREQUENCY DISTRIBUTION OF NORMALLY AERATED TISSUE AT DIFFERENT PLATEAU PRESSURES*

CT Scan Number (%)	Plateau Pressures		
	30 cm H_2O	35 cm H_2O	45 cm H_2O
−1000 − 900	0.04 ± 0.02	0.04 ± 0.01	0.06 ± 0.03
−900 − 800	3.38 ± 1.80	4.34 ± 2.22	5.48 ± 2.67
−800 − 700	15.48 ± 4.54	18.45 ± 4.59	20.11† ± 4.97
−700 − 600	18.94 ± 3.42	22.15† ± 3.36	24.42† ± 4.06
−600 − 500	19.67 ± 3.47	19.50 ± 4.26	18.32 ± 4.83

* Data were computed as a mean of the four experimental steps that reached the same inspiratory plateau pressure. Data are expressed as mean ± SEM.
† $p < 0.05$ compared with 30 cm H_2O plateau pressure.

The importance of superimposed pressure in causing the end-expiratory collapse is shown in Figure 10, which expresses the amount of nonaerated tissue per level as a function of the corresponding transalveolar pressure. When the transalveolar pressure is negative, that is, the superimposed pressure is less than the PEEP applied, the amount of nonaerated tissue is of similar magnitude, and independent from the previous end-inspiratory pressure. However, when the transalveolar pressure is positive, indicating that the superimposed pressure in a given lung level is greater then the PEEP applied, the amount of nonaerated tissue significantly increases, as a function of the previous end-inspiratory pressure.

Hemodynamics and Gas Exchange

Cardiac output (CO), pulmonary artery (Ppa), pulmonary wedge (Ppw), and central venous (Pcv) pressures are reported in Table 5. These remained substantially unmodified during the entire experiment. The only change recorded was an increase in cardiac output—and therefore in Ppa, Ppw, and

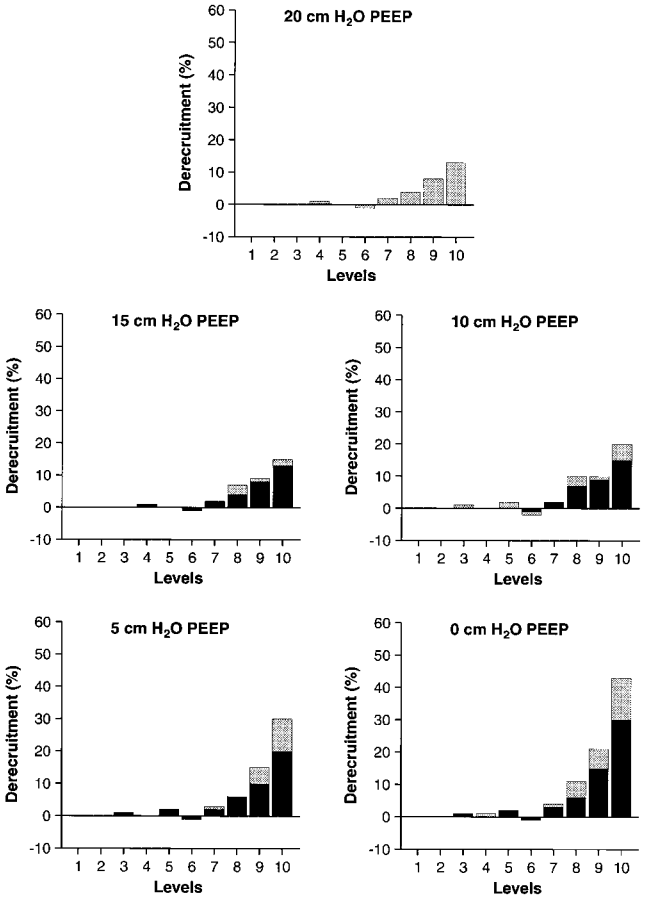

Figure 7. Regional pattern of derecruitment. Each graph shows fractional derecruitment as a function of lung levels (supine position, level 1 sternal, level 10 vertebral). *Gray bar chart* represents the incremental fractional derecruitment at different PEEP levels; *black bar chart* represents the fractional derecruitment obtained at the previous PEEP level. The *black bars* may present a lower value compared with a previous PEEP level, indicating a slight regional recruitment when decreasing airway pressure.

Pcv—at 20 cm H_2O of PEEP during 30 cm H_2O of plateau pressure, probably because of an increase in Pa_{CO_2} (from 51.6 ± 4.4 mm Hg to 65.9 ± 6.1 mm Hg, $p < 0.001$).

Gas exchange values are reported in Table 5. As shown, almost all these variables increased with PEEP, whatever plateau pressure was applied. It is noteworthy that the increases of Pa_{O_2} at the increase of PEEP were well correlated with the shift of poorly aerated tissue to aerated tissue ($r = 0.67$, $p < 0.001$, not shown).

Finally, Pa_{O_2} was positively but imprecisely correlated with the percentage of aerated tissue ($r = 0.55$, $p < 0.001$, not shown) and negatively correlated both with the percentage of poorly aerated tissue ($r = 0.58$, $p < 0.001$, not shown) and with the percentage amount of nonaerated tissue ($r = 0.48$, $p < 0.01$, not shown).

DISCUSSION

The main findings of this study were that in early ALI/ARDS (*1*) recruitment occurs along the entire VP curve of the respiratory system, even beyond the upper inflection point of the inspiratory VP relationship; (*2*) derecruitment is also a continuous process, but is most prevalent over a pressure range (0–10 cm H_2O) lower than the pressure range over which recruitment occurs; (*3*) there is an interaction between the extent of end-expiratory and end-inspiratory collapse; gravitational forces (i.e., the superimposed pressure) seem to play a substantial role in determining regional lung collapse; and (*4*) the most striking observation, however, was that despite the limited potential for recruitment of these patients, the "rules" for recruitment and derecruitment, the interactions between end-inspiratory and end-expiratory collapse, and the role of superimposed pressure appear impressively similar to those observed in a highly recruitable oleic acid model of acute lung injury (1).

Inflation and Recruitment

Over the past 20 years, several attempts have been made to utilize the VP curve of the respiratory system to select "optimal" ventilatory settings. After 1975, when Suter and coworkers introduced the "best PEEP" concept based on mechanical analysis of the respiratory system (13), subsequent efforts were initially directed toward PEEP selection. Since then, numerous studies have been published both in experimental and clinical subjects (14). Most of these studies concluded that because oxygenation improves with PEEP values higher than those corresponding to the lower inflection point, the latter should be used to titrate PEEP. This physiological concept was recently emphasized by Amato and coworkers, who showed that a lower inflection point-guided selection of PEEP was associated with increased survival (15). It is important, however, to stress the inference that "most recruitment" occurs around the lower inflection point region was drawn from oxygenation data, without any direct evidence. Moreover, this concept has been challenged both on the clinical evidence that additional oxygenation (and recruitment) may be obtained in some patients at PEEP levels well above those typically recorded for the lower inflection point (16, 17) and on a theoretical argument attempting to explain the contours of the composite VP curve (10, 11).

TABLE 4. NONAERATED TISSUE OF THE WHOLE CT SLICE AT DIFFERENT PLATEAU PRESSURES AND PEEP LEVELS*

Positive End-expiratory Pressure	Plateau pressures					
	30 cm H_2O		35 cm H_2O		45 cm H_2O	
	I	E	I	E	I	E
5 cm H_2O	6.22 ± 1.81	8.19‡ ± 2.03	5.49 ± 1.65	7.35‡ ± 1.85	4.53 ± 1.33	5.39 ± 1.60
10 cm H_2O	5.79 ± 1.80	6.38‡,§ ± 1.90	5.46 ± 1.68	6.66‡ ± 1.91	—	4.96 ± 1.54
15 cm H_2O	5.21† ± 1.73	6.09‡,§ ± 1.94	5.13 ± 1.56	5.75§ ± 1.76	—	4.55 ± 1.49
20 cm H_2O	5.40 ± 1.68	5.98‡,§ ± 1.80	4.76 ± 1.57	5.73§ ± 1.72	—	4.43 ± 1.39

Definition ofabbreviations: E = end expiration; I = end inspiration; PEEP = positive end-expiratory pressure.
* Single values of nonaerated tissue are expressed in grams. Data are expressed as mean ± SEM.
† $p < 0.05$ compared with 5 cm H_2O PEEP at the same plateau pressure for the end inspiration.
‡ $p < 0.05$ compared with 45 cm H_2O plateau pressure at the same PEEP level for end expiration.
§ $p < 0.05$ compared with 5 cm H_2O PEEPat the same plateau pressure for end expiration.

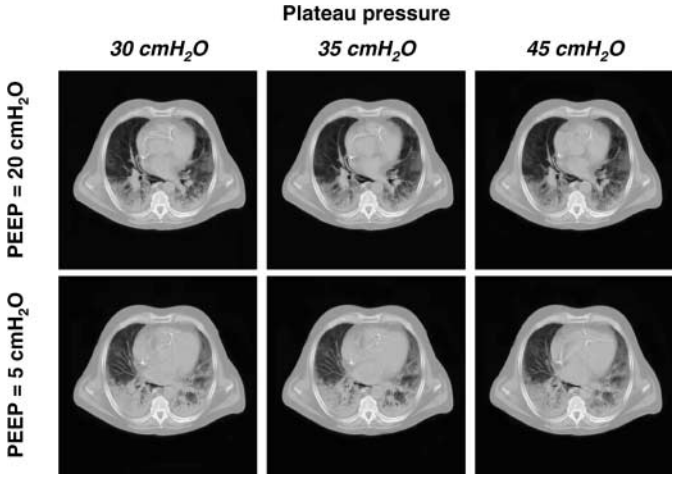

Figure 8. A representative CT scan obtained in one patient at end expiration for each experimental step. At a similar PEEP level, either 5 or 20 cm H_2O, the amount of end-expiratory collapse was dramatically different, depending on whether ventilation was performed at 30, 35, or 45 cm H_2O of plateau pressure.

In this study, we found that when assessed by CT scan, recruitment occurs continuously along the VP curve of the respiratory system, and that only a small fraction of the potential for recruitment is exploited at pressures below the lower inflection point. The data we obtained in patients are impressively similar to the data obtained in dogs with oleic acid-induced respiratory failure (1). Moreover, it is important to stress that this principle of continuous recruitment applies both when the potential for recruitment is very low (about 6% of the lung parenchyma in these series of patients), and when it is very high (about 50% in oleic acid dogs). Percent of inflation and percent of recruitment were parallel functions of applied pressure, both in oleic acid dogs and in ALI/ARDS patients. This suggests the potential use of the inspiratory VP curve as equivalent to a recruitment pressure curve, which indicates, at any given pressure, how much of the potential for recruitment has been exploited. Our data confirm with the CT scan the clinical findings of Jonson and coworkers (17) and the theoretical arguments proposed by Hickling (10) and Venegas and coworkers (11), who questioned the value of the lower inflection point as a marker of the end of recruitment. It is important to stress, however, that although the Hickling model assumed an uniform distribution of the estimated TOPs, we actually found a gaussian distribution, as suggested by Venegas and coworkers, with estimated TOPs ranging from 10 cm H_2O to 45 cm H_2O (the entire range of pressure we explored in human study) and from 10 cm H_2O to 60 cm H_2O in dogs (in which the achieved pressure ranged from 0 to 70 cm H_2O).

Apart from any gravitational consideration, the wide distribution of estimated TOPs may reflect the fundamentally different nature of the underlying atelectasis. It is known that the pressures needed to reverse collapse of the small airways are generally lower (10–20 cm H_2O) than the pressures required to reopen reabsorption atelectasis (18). The current study suggests that in ARDS, there exists a wide range of opening pressures, from 0 to infinite, through a continuum of "loose" and "sticky" forms of atelectasis, as previously speculated (19). This is emphasized by the analysis of estimated TOPs of single patient. In three of them (patients 1, 3, and 5), in fact, the prevalent atelectasis seems due to small airway collapse ("loose" atelectasis), whereas in two (patients 2 and 4), it seems due to true alveolar collapse ("sticky" atelectasis).

Moreover, our findings suggest that the different lung regions present different opening pressures (lowest in nondependent lung, intermediate in the mid lung, and highest in the most dependent lung). As shown in Figure 5, in the three most nondependent levels, no recruitment occurs, as no recruitable tissue exists; the recruitment is complete down to level 6–7 (2/3 of the lung) at an inspiratory pressure of 30 cm H_2O, and recruitment in the most dependent lung regions continues to occur at pressures as high as 45 cm H_2O. These data fit a "sponge" model of ALI/ARDS (20), in which atelectasis mainly occurs because of the gravitational forces generated by a uniformly edematous lung (compression atelectasis). It is tempting to speculate that the first three levels are open, as the gravitational forces are not sufficient to cause atelectasis. In the middle lung region, gravitational forces cause primarily small airway closure (opening pressure 20–30 cm H_2O), and in the

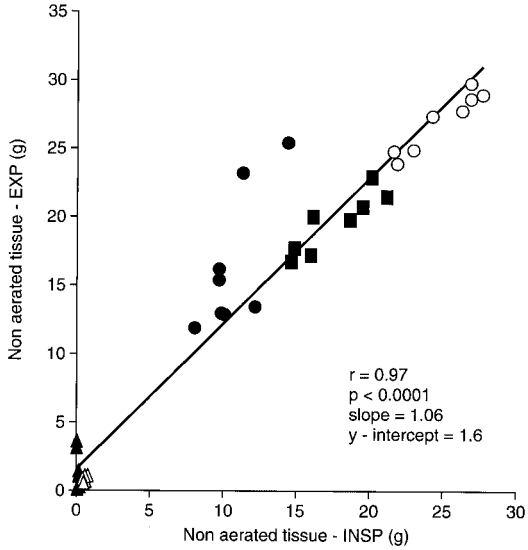

Figure 9. End-expiratory nonaerated tissue as a function of end-inspiratory nonaerated tissue. *Solid circles* refer to patient 1; *open circles* refer to patient 2; *solid triangles* refer to patient 3; *open triangles* refer to patient 4; *solid squares* refer to patient 5.

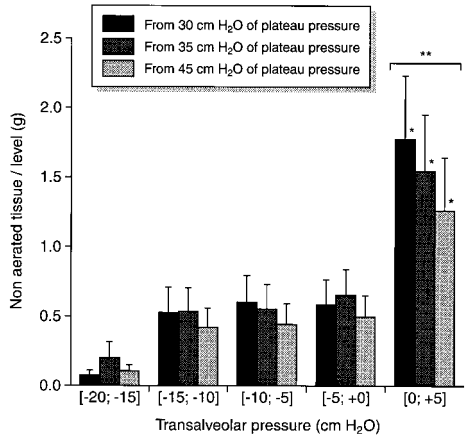

Figure 10. Nonaerated tissue, at end expiration, measured at each lung level as a function of the transalveolar pressure measured at that level. Data are expressed as mean ± SEM. *$p < 0.05$ compared with other transalveolar pressures coming from the same plateau pressure. **$p < 0.05$ compared with nonaerated tissue/level coming from other plateau pressures at the same transalveolar pressure.

TABLE 5. GAS EXCHANGE AND HEMODYNAMIC VARIABLES*

	Plateau Pressures							
	30 cm H_2O				35 cm H_2O			
PEEP (*cm* H_2O)	5	10	15	20	5	10	15	20
Ppa, mm Hg	$24.2^{\dagger,\ddagger} \pm 1.6$	$25.2^{\dagger} \pm 1.7$	$28.2^{\dagger} \pm 0.7$	$36.2^{\ddagger} \pm 2.6$	$21.2^{\dagger} \pm 1.0$	$22.81^{\dagger} \pm 2.1$	26.2 ± 1.8	31.2 ± 2.4
Pcv, mm Hg	$10.2^{\dagger} \pm 2.1$	$10.2^{\dagger} \pm 1.4$	$10.8^{\dagger} \pm 1.2$	14.4 ± 2.1	$9.5^{\dagger} \pm 2.1$	10.5 ± 1.2	11.1 ± 0.9	12.9 ± 1.8
Ppw, mm Hg	15.2 ± 2.6	15.8 ± 2.9	15.0 ± 2.7	17.0 ± 1.0	14.0 ± 1.9	15.8 ± 3.0	16.8 ± 2.7	16.0 ± 1.3
CO, L/min	$8.6^{\dagger} \pm 0.8$	$8.6^{\dagger,\ddagger} \pm 0.9$	8.9 ± 0.8	$10.4^{\ddagger} \pm 0.9$	8.6 ± 0.8	7.4 ± 0.9	8.0 ± 1.0	8.9 ± 0.9
Pa_{O_2}, mm Hg	$101.8^{\ddagger} \pm 5.6$	125.8 ± 6.1	141.4 ± 6.9	$122.8^{\ddagger} \pm 8.7$	$95.5^{\dagger,\S} \pm 6.3$	120.3 ± 5.2	135.3 ± 13.1	144.0 ± 12.5
Pv_{O_2}, mm Hg	$40.6^{\dagger} \pm 1.4$	$43.0^{\dagger} \pm 2.8$	$47.8^{\dagger} \pm 3.5$	58.2 ± 5.3	$38.0^{\dagger} \pm 0.6$	$39.5^{\dagger} \pm 2.0$	46.5 ± 1.4	53.8 ± 2.3
Pa_{CO_2}, mm Hg	$37.9^{\dagger,\S} \pm 2.7$	$42.4^{\dagger,\S} \pm 4.8$	$51.6^{\dagger,\ddagger} \pm 4.4$	$65.9^{\ddagger} \pm 6.1$	$32.8^{\dagger,\S} \pm 2.5$	$40.0^{\dagger} \pm 3.5$	$43.6^{\dagger} \pm 4.4$	53.9 ± 4.2
Pv_{CO_2}, mm Hg	$43.3^{\dagger,\S} \pm 2.7$	$47.4^{\dagger} \pm 5.0$	$55.0^{\dagger} \pm 4.1$	67.6 ± 7.1	$37.4^{\dagger} \pm 2.4$	$44.9^{\dagger} \pm 3.8$	46.4 ± 3.3	56.5 ± 3.7
V_T, L	$1.22^{\P,\ddagger} \pm 0.25$	$0.96^{\dagger} \pm 0.18$	$0.68^{\ddagger} \pm 0.16$	$0.43^{\ddagger} \pm 0.12$	$1.42^{\P} \pm 0.27$	$1.05^{\dagger} \pm 0.19$	$0.86^{\dagger} \pm 0.18$	0.55 ± 0.12
$\dot{V}_E$, L/min	$13.3^{\P,\ddagger} \pm 1.1$	$10.4^{\P,\ddagger} \pm 0.9$	$6.8^{\ddagger} \pm 0.5$	$4.0^{\P,\ddagger} \pm 0.4$	$16.4^{\P} \pm 1.8$	$12.1^{\P} \pm 1.2$	$9.3^{\P} \pm 1.1$	$5.8^{\P} \pm 0.6$

Definition of abbreviations: CO = cardiac output; Pcv = central venous pressure; PEEP = positive end-expiratory pressure; Ppa = mean pulmonary artery pressure; Ppw = pulmonary wedge pressure; $\dot{V}_E$ = minute ventilation; V_T = tidal volume.

* Data are expressed as mean ± SEM.

† $p < 0.05$ compared with 20 cm H_2O PEEP at the same plateau pressure.

‡ $p < 0.05$ compared with 35 cm H_2O plateau pressure at the same PEEP level.

§ $p < 0.05$ compared with 15 cm H_2O PEEP at the same plateau pressure.

¶ $p < 0.05$ compared with other PEEP levels at the same plateau pressure.

most dependent lung region, there is a prevalence of reabsorption atelectasis (opening pressures 30–45 cm H_2O). The prevalence of reabsorption atelectasis in this lung regions may also be explained in the supine position by heart weight (21) and abdominal pressure (22), as well as by superimposed pressure. All these factors tend to decrease the transpulmonary pressure, thus enhancing the possibility of true alveolar collapse. The absolute amount of atelectasis, of course, may vary according to underlying pathology, or pathogenetic pathway (consolidation versus collapse). However, independent of the absolute amount of atelectasis (i.e., the potential for recruitment) the processes of opening appear to be the same, both in ALI/ARDS and in our experimental oleic acid model (1).

Hyperinflation and Overstretching

It has been claimed that the CT scan may be a useful tool for detecting hyperinflation in ARDS (8). Unfortunately, the term "hyperinflation" is often used as if it were synonymous with "overstretching," whereas the two terms define different concepts. Strictly speaking, hyperinflation is a situation in which the ratio of gas to tissue is higher than normal (i.e., in CT scan technology, the percentage of voxels included in the compartment between −900 HU [= gas tissue ratio of 9/1] and −1000 HU [all gas]). The typical example is emphysema, as described several years ago (23). Overstretching, however, defines a situation in which the distending pressure is abnormally elevated, that is, an abnormally increased alveolar wall tension, and this phenomenon may occur in the absence of hyperinflation, as previously defined. In fact, the overall density (i.e., the ratio of tissue to the sum of gas and tissue in a given voxel) is elevated in ALI/ARDS, due to the increase of "tissue" content, and to the decrease of gas content. Increasing airway pressure to the flatter portion of the VP curve (up to 45 cm H_2O, as in our study—*see* Figure 2) may cause overstretching without inducing hyperinflation, simply because the tissue mass is high enough to prevent the achievement of a gas tissue ratio greater than 9/1. In fact, as in previous studies (12), we did not find any "hyperinflation," even at 45 cm H_2O inspiratory pressure, a condition in which overstretching was likely to be present (*see* Figure 2 and Table 3). Indeed, we believe that although CT scan may detect hyperinflation in other settings, it may not effectively detect either overstretching or hyperinflation in conditions of diffusely increased tissue mass.

Deflation and Derecruitment

Although recruitment and inflation follow the same pattern, and are highly correlated, we found that in this series of ALI/ARDS patients derecruitment is partially dissociated from deflation. The majority of the derecruitment occurs at PEEP values spanning 0 to 15 cm H_2O (i.e., in the range of superimposed pressure).

At a given airway pressure, the amount of gas is higher during deflation, as illustrated in our recruitment and derecruitment pressure curves (*see* Figures 3 and 6). At the same pressure of 10 cm H_2O, only 15% of the collapsed tissue has been opened on the inspiratory limb, whereas 50% remains open on the deflation limb. These findings, as we will discuss later, cast doubt on the utility of using the inspiratory limb of the VP curve to set PEEP, which is an expiratory and not an inspiratory maneuver. Derecruitment appears to follow, as does recruitment, a defined spatial pattern (*see* Figure 7). Decreasing the PEEP level from TLC caused progressive collapse of the most dependent regions, which are subjected to the greatest superimposed pressure. Of note, no derecruitment was observed in the first three to four least dependent levels at any level of PEEP.

Interactions between End-inspiratory and End-expiratory Lung Collapse

As in oleic acid-injured dogs, we found that the extent of end-expiratory collapse differs at the same PEEP level, depending on the previous inspiratory history, and that there is a straightforward direct correlation between the extents of end-expiratory and end-inspiratory collapse. Moreover, as in oleic acid-injured dogs, the superimposed pressure seems to play a substantial role in determining the extent of end-expiratory collapse. In fact, when the transalveolar pressure is positive, the lung cannot stay open, independent of the previous inspiratory history.

Gas Exchange

End-expiratory collapse related inversely to Pa_{O_2}, as previously observed (12), emphasizing that the CT data truly reflect the underlying conditions, which dictate the severity of the respiratory failure.

Possible Clinical Implications

Some of these findings may apply to clinical practice. First, our results confirm that recruitment is a pan-inspiratory phe-

nomenon that is not delimited by the inflection/deflection regions of the inflation limb of the respiratory VP curve. Because the range of opening pressure is extremely wide, it follows that if one believes that "opening" the lung is beneficial in terms of lung protection, a maneuver intended to fully recruit the lung requires pressures higher than 35 cm H_2O in the supine position. Data from the current clinical study are consistent with what we previously found using sighs of 45 cm H_2O (19). It is very likely that pressures higher than 45 cm H_2O may be needed for effective recruitment maneuvers in supine patients, especially in the presence of increased chest wall elastance (24).

Recruited lung units tend to stay open at pressures lower than those that opened them. We found, both in ALI/ARDS patients and in oleic acid-injured dogs, that collapse maximally occurs between 0 and 15 cm H_2O, reinforcing the role of the superimposed pressure. From this standpoint, thoracic shape (i.e., the sternal–vertebral dimension) might be worth considering when estimating the PEEP needed to "keep the lung open."

Our data do not provide any information regarding the maintenance of recruitment over time. Previous work suggests that establishing adequate regional V_A/Q ratios may play a substantial role in maintaining open what has been recruited, by preventing the appearance of the reabsorption atelectasis (19).

From clinical and experimental evidence, we now know that tidal volumes, which repeatedly encroach on the lung expansion limits, should be avoided (25), and that lung collapse and reopening that occur throughout the respiratory cycle are likely to be injurious (26). We lack evidence, however, that allowing the airway to remain closed is dangerous. In providing insight regarding the mechanics of recruitment and derecruitment in the early phase of ARDS, our data may be of clinical relevance if one believes that preventing lung collapse is a worthy strategy. The importance of this "open lung" ventilation on long-term outcomes remains to be proved.

References

1. Pelosi P, Goldner M, McKibben A, Adams A, Eccher G, Caironi P, Losappio S, Gattinoni L, Marini JJ. Recruitment and derecruitment during acute respiratory failure. An experimental study. *Am J Respir Crit Care Med* 2001;164:122–130.
2. Gattinoni L, Pelosi P, Suter PM, Pedoto A, Vercesi P, Lissoni A. Acute respiratory distress syndrome caused by pulmonary and extrapulmonary disease. Different syndrome? *Am J Respir Crit Care Med* 1998;158:3–11.
3. Terashima T, Matsubara H, Nakamura M, Sakamaki F, Waki Y, Soejima K, Tasaka S, Hidetoshi N, Sayama K, Ishizaka A, Kanazawa M. Local *Pseudomonas* instillation induces controlateral lung injury and plasma cytokines. *Am J Respir Crit Care Med* 1996;153:1600–1605.
4. Bernard BG, Artigas A, Brigham KL, Carlet J, Falke K, Hudson L, Lamy M, Legall JR, Morris A, Spragg R, and the Consensus Committee. The American-European Consensus Conference on ARDS. Definitions, mechanisms, relevant outcomes, and clinical trial coordination. *Am J Respir Crit Care Med* 1994;149:818–824.
5. Gattinoni L, Pesenti A, Avalli L, Rossi F, Bombino M. Pressure-volume curve of total respiratory system in acute respiratory failure. *Am Rev Respir Dis* 1987;136:730–736.
6. Damia G, Mascheroni D, Croci M, Tarenzi L. Perioperative changes in functional residual capacity in morbidly obese patients. *Br J Anaesth* 1988;60:574–578.
7. Gattinoni L, Pelosi P, Crotti S, Valenza F. Effects of positive end-expiratory pressure on regional distribution of tidal volume and recruitment in adult respiratory distress syndrome. *Am J Respir Crit Care Med* 1995; 151:1807–1814.
8. Vieira SRR, Puybasset L, Richecoeur J, Lu Q, Cluzel P, Gusman PB, Coriat P, Rouby JJ. A lung computed tomographic assessment of positive end-expiratory pressure-induced lung overdistention. *Am J Respir Crit Care Med* 1998;158:1571–1577.
9. Pelosi P, D'Andrea L, Vitali G, Pesenti A, Gattinoni L. Vertical gradient of regional lung inflation in adult respiratory distress syndrome. *Am J Respir Crit Care Med* 1994;149:8–13.
10. Hickling KG. The pressure-volume curve is greatly modified by recruitment. A mathematical model of ARDS lungs. *Am J Respir Crit Care Med* 1998;158:194–202.
11. Venegas JG, Harris RS, Simon BA. A comprehensive equation for the pulmonary pressure-volume curve. *J Appl Physiol* 1998;84:389–395.
12. Gattinoni L, Pesenti A, Bombino M, Baglioni S, Rivolta M, Rossi F, Rossi G, Fumagalli R, Marcolin R, Mascheroni D, Torresin A. Relationships between lung computed tomographic density, gas exchange, and PEEP in acute respiratory failure. *Anesthesiology* 1988;69:824–832.
13. Suter PM, Fairley B, Isemberg MD. Optimum end-expiratory airway pressure in patients with acute pulmonary failure. *N Engl J Med* 1975;292:284–289.
14. Beydon L, Lemaire F, Jonson B. Lung mechanics in ARDS. Compliance and pressure-volume curve. In: Zapol M, Lemaire F, editors. Adult respiratory distress syndrome. New York: Marcel Dekker; 1991. p. 139–161.
15. Amato MB, Barbas CS, Medeiros DM, Magaldi RB, Schettino GP, Lorenzi-Filho G, Kairalla RA, Deheinzelin D, Munoz C, Oliveira R, Takagaki TY, Carvalho CRR. Effect of a protective-ventilation strategy on mortality in the acute respiratory distress syndrome. *N Engl J Med* 1998;338:347–354.
16. Kirby RR, Downs JB, Civetta JM. High level positive end expiratory pressure (PEEP) in acute respiratory insufficiency. *Chest* 1975;67:156–163.
17. Jonson B, Richard JC, Straus C, Mancebo J, Lemaire F, Brochard L. Pressure-volume curves and compliance in acute lung injury. Evidence of recruitment above the lower inflection point. *Am J Respir Crit Care Med* 1999;159:1172–1178.
18. Glaister DH, Schroter RC, Sudlow MF, Milic-Emili J. Transpulmonary pressure gradient and ventilation distribution in excised lungs. *Respir Physiol* 1973;17:365–385.
19. Pelosi P, Cadringher P, Bottino N, Panigada M, Carrieri F, Riva E, Lissoni A, Gattinoni L. Sigh in Acute Respiratory Distress Syndrome. *Am J Respir Crit Care Med* 1999;159:872–880.
20. Bone RC. The ARDS lung. New insights form computed tomography. *JAMA* 1993;269:2134–2135.
21. Malbouisson LM, Busch CJ, Puybasset L, Lu Q, Cluzel P, Rouby JJ, and the CT Scan ARDS Study Group. Role of the heart in the loss of aeration characterizing lower lobes in acute respiratory distress Syndrome. *Am J Respir Crit Care Med* 2000;161:2005–2012.
22. Albert RK, Hubmayr RD. The prone position eliminates compression of the lungs by the hearth. *Am J Respir Crit Care Med* 2000;161:1660–1665.
23. Hayhurst MD, MacNee W, Flenley DC, Wright D, McLean A, Lamb D, Wightman AJ, Best J. Diagnosis of pulmonary emphysema by computerised tomography. *Lancet* 1984;11:320–322.
24. Mergoni M, Martelli A, Volpi A, Primavera S, Zuccoli P, Rossi A. Impact of positive end-expiratory pressure on chest wall and lung pressure-volume curve in acute respiratory failure. *Am J Respir Crit Care Med* 1997;156:846–854.
25. The Acute Respiratory Distress Syndrome Network. Ventilation with lower tidal volumes as compared with traditional tidal volumes for acute lung injury and the acute respiratory distress syndrome. *N Engl J Med* 2000;342:1301–1308.
26. Muscedere JG, Mullen JBM, Gan K, Slutsky AS. Tidal ventilation at low airway pressures can augment lung injury. *Am J Respir Crit Care Med* 1994;149:1327–1334.